

University of Mississippi

eGrove

Honors Theses


Honors College (Sally McDonnell Barksdale
Honors College)

Spring 5-8-2020

Design and Synthesis of Novel Analogs as Potential Antitubercular Agents

Peggy McCluggage

Follow this and additional works at: https://egrove.olemiss.edu/hon_thesis

 Part of the [Medicinal Chemistry and Pharmaceutics Commons](#), [Other Immunology and Infectious Disease Commons](#), and the [Pharmaceutical Preparations Commons](#)

Recommended Citation

McCluggage, Peggy, "Design and Synthesis of Novel Analogs as Potential Antitubercular Agents" (2020). *Honors Theses*. 1572.

https://egrove.olemiss.edu/hon_thesis/1572

This Undergraduate Thesis is brought to you for free and open access by the Honors College (Sally McDonnell Barksdale Honors College) at eGrove. It has been accepted for inclusion in Honors Theses by an authorized administrator of eGrove. For more information, please contact egrove@olemiss.edu.

Design and Synthesis of Novel Analogs as Potential Antitubercular Agents

by
Peggy Ann McCluggage

A thesis submitted to the faculty of The University of Mississippi in partial fulfillment of
the requirements of the Sally McDonnell Barksdale Honors College.

Oxford, MS
2020

Approved by

Advisor: Professor Sudeshna Roy, Ph.D.

Reader: Professor Susan Pedigo, Ph.D.

Reader: Professor Randy Wadkins, Ph.D.

© 2020
Peggy Ann McCluggage
ALL RIGHTS RESERVED

ACKNOWLEDGMENT

I would first like to thank Dr. Sudeshna Roy whose enthusiasm about research and knowledge first drew me to her lab. She has pushed me not only as a scientist but also as a member of society, and this project would not have been possible without her guidance and patience. I would also like to thank my second reader Dr. Susan Pedigo who has inspired much of my curiosity within and outside of science and my third reader Dr. Randy Wadkins. In addition, I would like to thank the other members of Roy laboratory who have been like family the last couple of years as well as my actual friends and family. I am especially grateful for my mom and dad who have never doubted my abilities but encourage me to use them to pursue my passions. Finally, I would like to thank the Department of Biomolecular Sciences and the Sally McDonnell Barksdale Honors College for supporting this project.

ABSTRACT

Tuberculosis (TB) is an infectious, airborne disease which primarily infects the lungs. One-third of the world's population is currently estimated to be infected with *Mycobacterium tuberculosis* (Mtb), the causative agent for TB [1]. Current treatment for this disease requires at least six months of taking multiple antibiotics with undesirable side effects [2]. Difficulty in complying to this regimen as well as the prevalence of HIV/AIDS has led to antimicrobial resistance seen in Mtb. In order to combat the Multi-Drug Resistant and Extensively-Drug Resistant strains of the disease-causing bacteria, preventative care and novel antibiotics are urgently needed [3]. The purpose for this research is to design and synthesize novel and improved analogs as potential antitubercular agents. One promising new target explored was the protein phospho-MurNAc-pentapeptide translocase (MraY) responsible for the biosynthesis of peptidoglycan in the cell wall of Mtb [4]. Two narrow-spectrum analogs were designed and synthesized with the collaboration of other lab members, and initial testing showed that neither was active against Mtb.

While the MraY project was being pursued, other members of Roy lab were developing regioselective synthetic methods for 4-fluoro-1,5- disubstituted-1,2,3-triazoles. A paper by Patpi et al showed that 1,2,3-triazoles combined with dibenzothiophene through a molecular hybridization approach led to the synthesis of analogs with promising antitubercular activity. Because of the potential increased pharmacokinetic properties fluorine can provide, the second part of this project sought to create fluorinated versions of these analogs. To create the fluorinated analogs, an α -fluoronitroalkene would be reacted with an azide to cyclize to the final product. While

the azide was synthesized, the α -fluoronitroalkene moiety was not synthesized as a result of time restrictions caused by the COVID-19 pandemic. After the synthesis of these analogs is completed, they can be tested for antitubercular activity and, hopefully, contribute to the fight to slow antimicrobial resistance.

TABLE OF CONTENTS

ACKNOWLEDGMENT	iii
ABSTRACT	iv
LIST OF TABLES AND FIGURES	vii
LIST OF ABBREVIATIONS	viii
CHAPTER 1: INTRODUCTION & BACKGROUND	1
SECTION 1.1 – INTRODUCTION TO TUBERCULOSIS.....	1
SECTION 1.2 – <i>MYCOBACTERIUM TUBERCULOSIS</i> AND ANTIMICROBIAL RESISTANCE	2
CHAPTER 2: DESIGN AND SYNTHESIS OF ANALOGS TARGETING MRAY 10	
SECTION 2.1 – LITERATURE PRECEDENTS AND PROPOSED PROJECT.....	10
SECTION 2.2 – RESULTS AND DISCUSSION	13
SECTION 2.3 – CONCLUSION AND FUTURE WORK	16
SECTION 2.4 – CHARACTERIZATION DATA AND SYNTHETIC SCHEMES.....	17
CHAPTER 3: FLUORINATED TRIAZOLES IN ANTITUBERCULAR ANALOGS	22
SECTION 3.1 – LITERATURE PRECEDENT AND PROPOSED PROJECT	22
SECTION 3.2 – RESULTS AND DISCUSSION	24
SECTION 3.3 – CONCLUSION AND FUTURE WORK	25
SECTION 3.4 – CHARACTERIZATION DATA (H^1 NMR).....	26
CHAPTER 4: SUPPLEMENTAL INFORMATION	29
SECTION 4.1 – REFERENCES.....	29

LIST OF TABLES & FIGURES

Chapter 1 –

Figure 1. The human immune response to Mtb (Nunes-Alvez, 2016)	3
Figure 2. First-line TB therapy (Nahid, 2016)	6
Figure 3. Antitubercular drugs and their targets (Goldberg, 2012)	6
Figure 4. Second-line TB therapy (Goldberg, 2012)	7

Chapter 2 –

Figure 5. MraY in Lipid I synthesis (Chung, 2016)	10
Table 1. Docking Scores of CAP6 and CAP7	12

LIST OF ABBREVIATIONS

AMR	Antimicrobial resistance
BSA	Bis(trimethylsilyl) acetamide
DAST	Diethylaminosulfur trifluoride
DBU	1,8-Diazabicyclo [5.4.0] undec-7-ene
DCM	Dichloromethane
DMF	Dimethylformamide
DPPA	Diphenyl pho
HIV/AIDS	Human immunodeficiency virus/Acquired immune deficiency syndrome
MD2	Muraymycin D2
MDR	Multi-drug resistant
MraY	phospho-MurNAc-pentapeptide translocase
Mtb	<i>Mycobacterium tuberculosis</i>
NMR	Nuclear magnetic resonance
Pyr	Pyridine
RIPE	Rifampicin, isoniazid, pyrazinamide, ethambutol
rt	Room temperature
STR	Streptomycin
TB	Tuberculosis
TBAI	Tetrabutylammonium iodide
TEA	Triethyl amine
TFA	Trifluoroacetic acid
THF	Tetrahydrofuran
UM5A	UDP-MurNAc-pentapeptide
XDR	Extensively drug resistant

Chapter 1: Introduction & Background

Section 1.1 – Introduction to tuberculosis

History of tuberculosis and current epidemic

In many ways, humans are disconnected from their origins and much of their history. Fossil records can be studied, and they show a glimpse of what ancient humans experienced; but, with the progression of human languages, technologies, and understanding of the world, there is very little that connects the current human experience to the experiences of ancient humans. To find common ground, one can look at infectious diseases—especially those which have coevolved with humans and which have yet to be overcome—such as tuberculosis (TB) caused by the pathogen *Mycobacterium tuberculosis* (Mtb).

Research suggests that the common ancestor of Mtb as it is known today may have appeared 15,000-20,000 years ago. The origins of Mtb go back even further. *Mycobacteria* likely originated 150 million years ago, and three million years ago East African hominids may have been infected by an early progenitor of Mtb. As Mtb evolved, so did human understanding and names of the disease it caused. From the name “phthisis” in Ancient Greece to the names “consumption” and the “white plague”, many names were based on the symptoms caused by Mtb. These included the general wasting away and consumption patients faced as well as the pallor that was characteristic of the disease. These and other names were used to refer to this disease until Johann Lukas Schönlein gave the name “tuberculosis” in the mid-19th century in reference to the “tubercles” or nodular lesions most commonly appearing on the lungs of those infected. Additionally, around this time the clinical symptoms of TB were recognized and defined

as a prolonged cough, difficulty breathing, and coughing up of mucus that contains bacteria [6].

While in countries such as the United States this “white plague” may feel as far in humanity’s past as the Black Plague, the reality is that an estimated one-third of the world’s population is infected by Mtb. Of those infected, one in ten will experience the active form of the disease, leaving the other 90% with an inactive, latent form of the infection to be discussed in more detail shortly. While these odds may not sound terrible, one-third of the world’s 7.8 billion people is 2.6 billion people; so, 260 million people are estimated to have the active form of this disease, and, in fact, infection by Mtb is currently the leading cause of death by a single infectious disease worldwide.

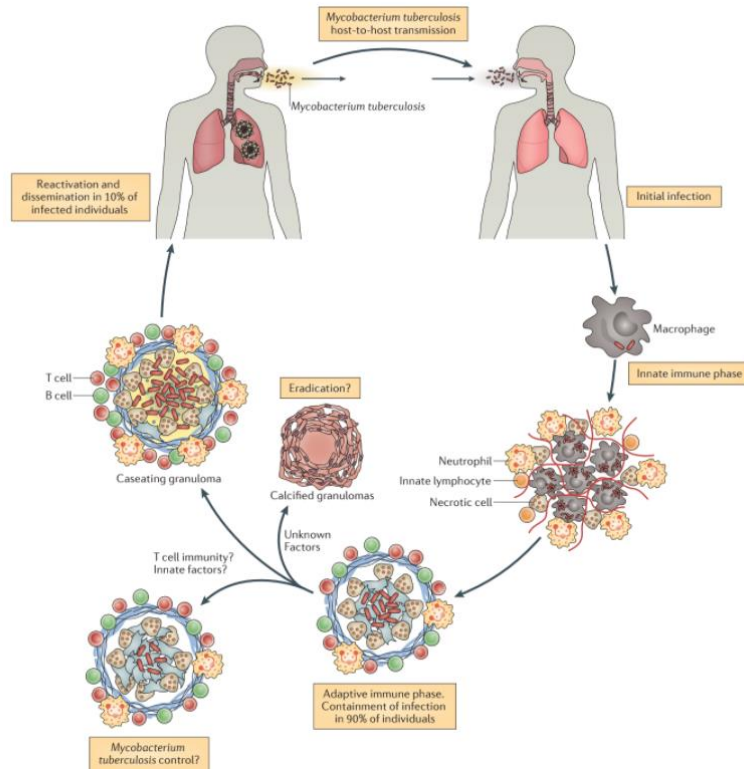
Second in total death toll to TB is HIV/AIDS, and research has shown a concerning connection between HIV/AIDS and the outcome of TB infection. Tuberculosis took the lives of 1.5 million people in 2018—of those, 251,000 were coinfecting with HIV. While incidence of TB cases in the United States has hit a record low, the decline is marginal in other countries. Of the estimated 10 million new TB cases in 2018, about two-thirds were in the following eight countries: India, China, Indonesia, the Philippines, Pakistan, Nigeria, Bangladesh, and South Africa. Coinfection of HIV and TB as well as antimicrobial resistance (AMR), to be discussed in more detail shortly, have greatly contributed to the epidemic of TB as it currently stands [3].

Section 1.2 – *Mycobacterium tuberculosis* and antimicrobial resistance

Human immune response to Mtb

As previously mentioned, only 10% of those infected with Mtb will have the active form of TB. The other 90% will be left with an inactive, latent form of the

infection. While latent TB is not infectious and does not present problems to the host, latent TB is another large obstacle in the way of accomplishing the World Health Organization's goal of ending the TB epidemic by the year 2030 [3]. By looking at the immune response to Mtb, latent TB and the challenges it presents can be more clearly understood. As an airborne pathogen, Mtb is spread through aerosol droplets by



coughing, sneezing, or spitting and can live in the air for several hours [7]. As is seen in **Figure 1**, the innate immune response is deployed first and with less specificity to Mtb compared to the adaptive immune response that follows.

Figure 1: The human immune response to Mtb begins after it is transmitted through droplets, then the innate response begins before the adaptive response contains the bacteria in granulomas [1].

While Mtb can infect other organs of the

body, it primarily infects the lungs; so, the innate immune response brings inflammatory cells to the lungs. Dendritic cells in the lymphatic system find and pick up Mtb and carry it to the lymph nodes where the Mtb is presented, and the body can prepare an adaptive immune response. After their activation and migration, antigen-specific (in this case, Mtb-specific) T-cells work with other leukocytes to contain the Mtb in granulomas. These

granulomas contain macrophages which are phagocytic cells capable of absorbing the bacteria. The macrophages work with other lymphocytes and fibroblasts which provide structural support as they are the most common cells found in connective tissues. For most, Mtb will remain contained in the granulomas; for a small portion of those infected, the disease will progress to its active form releasing Mtb from the granulomas. Those on medications for autoimmune diseases are especially at risk. While the suppression of parts of the immune system is important for these diseases including HIV/AIDS, this also suppresses the body's ability to contain Mtb and can lead to activation of latent TB in these patients [1].

Characterization of Mycobacterium tuberculosis and current therapy

On March 24, 1882 Robert Koch presented his Nobel Prize-winning work of identifying, isolating, cultivating and reproducing TB by inoculation of laboratory animals [6]. There are many characteristics of Mtb which distinguish it from other bacteria and make it a difficult pathogen to kill. Most bacteria can be categorized as either gram-positive or gram-negative. Both have an inner membrane; however, the key difference between the two is that gram-negative bacteria have a much thinner layer of peptidoglycan and have an additional outer membrane which prevents Gram iodine solution from binding with its thin layer of peptidoglycan. Gram-positive bacteria have a thick layer of peptidoglycan— a mesh-like protective layer made up of repeating units of sugars and amino acids— which is easily accessible and dyed by Gram iodine stain. To visualize gram-negative bacteria, a decolorizer is added which dissolves the outer membrane of gram-negative bacteria allowing the bacteria to be dyed by a lighter counterstain such as safranin without disturbing the dyed gram-positive cells [8].

Mycobacteria have a unique cell wall which makes them neither gram-positive nor gram-negative.

While *Mycobacteria* have a peptidoglycan layer comparable to that of gram-negative bacteria, their outer cell membrane is much thicker; the outer membrane is anchored by mycolic acids which are branched long chain fatty acids connected to a layer of arabinogalactan which can be seen in **Figure 3**. The complexity of the outer membrane and high presence of lipids relative to gram-negative bacteria prevents the outer membrane of *Mycobacteria* from being dissolved by a decolorizer or being dyed by a counterstain [9]. This difficulty in penetrating the cell for classification purposes also presents significant challenges in the development of antitubercular drugs.

Antimicrobial Resistance and current TB treatment

In 1933, the first synthesized antibiotic, Prontosil, which contained sulfanilamide, was used to successfully treat staphylococcal septicemia in a young, dying boy. Two years later, researchers learned that sulfanilamide was metabolized to sulphonamide, removed the dye from Prontosil, and thus began the sulphonamide era. This discovery along with the discovery of Penicillin began the 20-year period of antibiotic discovery now known as the Golden Age. With the end of the Golden Age came the beginning of a new era of antimicrobial resistance (AMR). Antitubercular drugs have been far from an exception to the persistence of antimicrobial resistance [10].

Streptomycin (STR) was the first antitubercular drug and, as such, set a trend for the future of antitubercular drugs and the resistance they would confer. The potential of STR to treat TB was discovered by Schatz in 1944, and the drug was used in humans two years later with great efficacy. Very shortly after its introduction, resistance was found in

more than 85% of cases making STR no longer an effective treatment. The need for combination therapy to slow the rapid evolution of resistance became apparent shortly after. The current treatment for TB consists of four drugs—rifampicin, isoniazid, pyrazinamide, and ethambutol—collectively known as RIPE therapy shown in **Figure 2**.

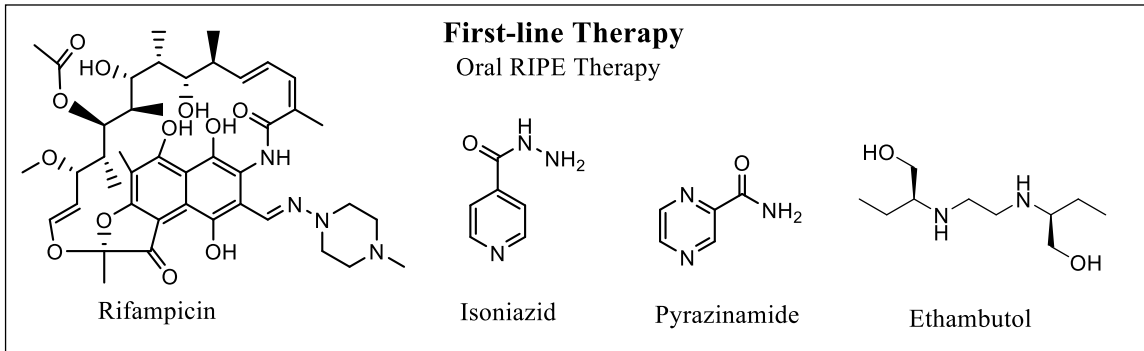


Figure 2: The first-line treatment for TB consists of the four drugs rifampicin, isoniazid, pyrazinamide, and ethambutol and is collectively known as RIPE therapy [2].

As is shown in **Figure 3**, the four drugs are used together because they each have a different target in Mtb: rifampicin inhibits transcription by targeting RNA polymerase and isoniazid and ethambutol inhibit cell wall synthesis by inhibiting the synthesis of mycolic acids and lipoarabinomannan respectively [11]. Recently, pyrazinamide has been shown to degrade aspartate decarboxylase PanD thus inhibiting biosynthesis of coenzyme A [12]. Standardly, the four drugs are taken for 2

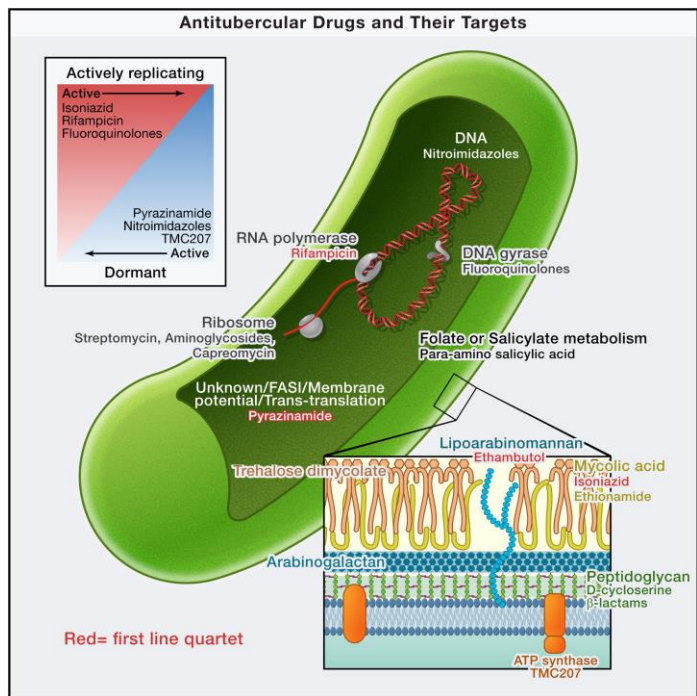


Figure 3: Antitubercular drugs, both first-line and second-line have different targets. The genes responsible for each enzyme can mutate and confer hereditary resistance [11].

months, followed by 4 months of rifampicin and isoniazid, the strongest of the 4 drugs. RIPE therapy has been used for over 40 years; however, this treatment does present problems. The drugs cause side effects and, as is common for many antibiotics, patients often stop taking them when they start to feel better. The 6 month-long treatment using 4 different drugs requires patient adherence, and this is a factor that is difficult to control. By not taking their antibiotic regimen all the way through, patients put themselves and others in danger. When the correct dosage is not taken consistently, selective pressure allows the Mtb which have mutations in the genes for the drug-targeted enzymes the opportunity to confer resistance to the drug they are exposed to, and thus future generations will receive this resistance. This is a large contribution to the current epidemic of TB [11].

As may have been anticipated, the resistance seen in Mtb is complex. The first category of resistant TB is multi-drug resistant (MDR) TB and is defined as Mtb that is resistant to and therefore cannot be treated by the 2 stronger drugs of RIPE therapy: rifampicin and isoniazid. To combat MDR TB, a variety of second-line therapeutics as shown in **Figure 4** are used. These drugs also have varying targets. As is shown in **Figure 3**, aminoglycosides inhibit translation by targeting ribosomes, fluoroquinolones inhibit replication by targeting DNA gyrase, *para*-aminosalicylic acid inhibits folate or salicylic acid metabolism, and prothionamide functions like ethionamide inhibiting cell wall biosynthesis by inhibiting the synthesis of mycolic acids. The next category of drug-resistant TB is extensively drug-resistant (XDR) TB. XDR TB is resistant to at least one injectable agent as well as one fluoroquinolone [11].

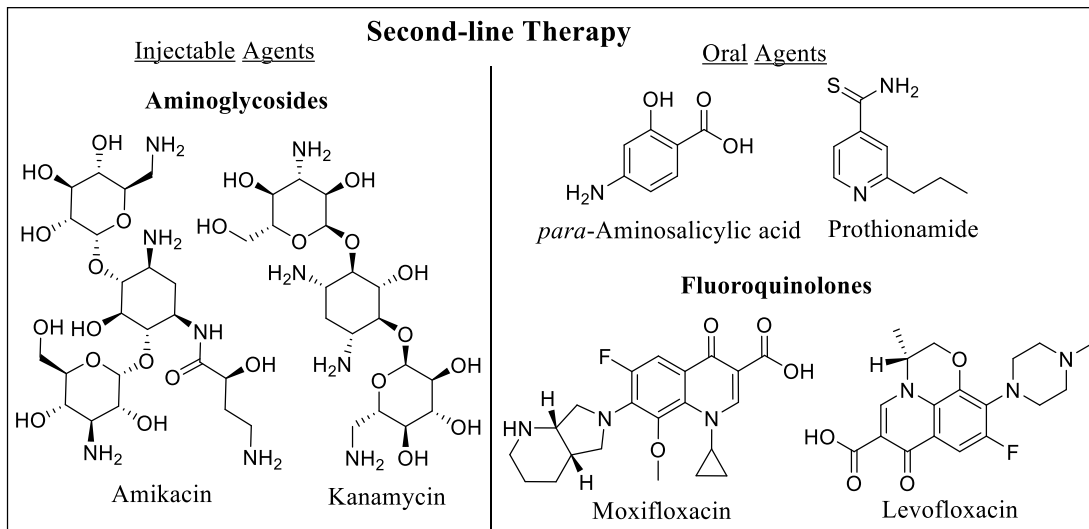


Figure 4: The second-line therapy for the treatment of MDR TB consists of a combination of injectable agents and oral agents [11]

An additional but possibly even more concerning contribution to drug resistant TB is its connection to patients infected by HIV. As was stated previously, the medications taken by patients with autoimmune diseases decrease the efficacy of the human immune response to TB. To add to this problem, studies have also shown that drug resistance is conferred in mice which are immune-deficient, and RIPE therapy interferes with the efficacy of antiretroviral treatment of HIV [11]. These factors contribute greatly to the large proportion of TB-related deaths in patients coinfecting with HIV and leave a great amount of space for improvement in TB treatment.

The BCG vaccine and need for new TB treatment

Currently, the only form of preventative care for TB is the Bacille Calmette-Guérin (BCG) vaccine. This vaccine was created from an isolated strain of *Mycobacterium bovis* and has been used in various parts of the world since the 1920's. As a result of varying methodology for making the vaccine, many strains of the BCG vaccine now exist [13]. The variable substrains used as well as differing policies per country have left the efficacy of BCG largely unknown and controversial. The vaccine

has proven mostly efficacious in the prevention of severe forms of TB on children such as TB meningitis, but the same cannot be concluded for adults [14]. The lack of preventative treatment and the persistence of resistant strains of TB have created the need for new TB therapeutics. New antibiotics are needed to counter MDR and XDR TB by exploiting new targets in Mtb and improving upon analogs with antitubercular activity.

Chapter 2: Design and synthesis of analogs targeting *MraY*

Section 2.1 – Literature precedents and proposed project

One promising target for antibiotic design is phospho-MurNac-pentapeptide translocase (*MraY*). As was shown in Chapter 1, many current antibiotics target cell wall

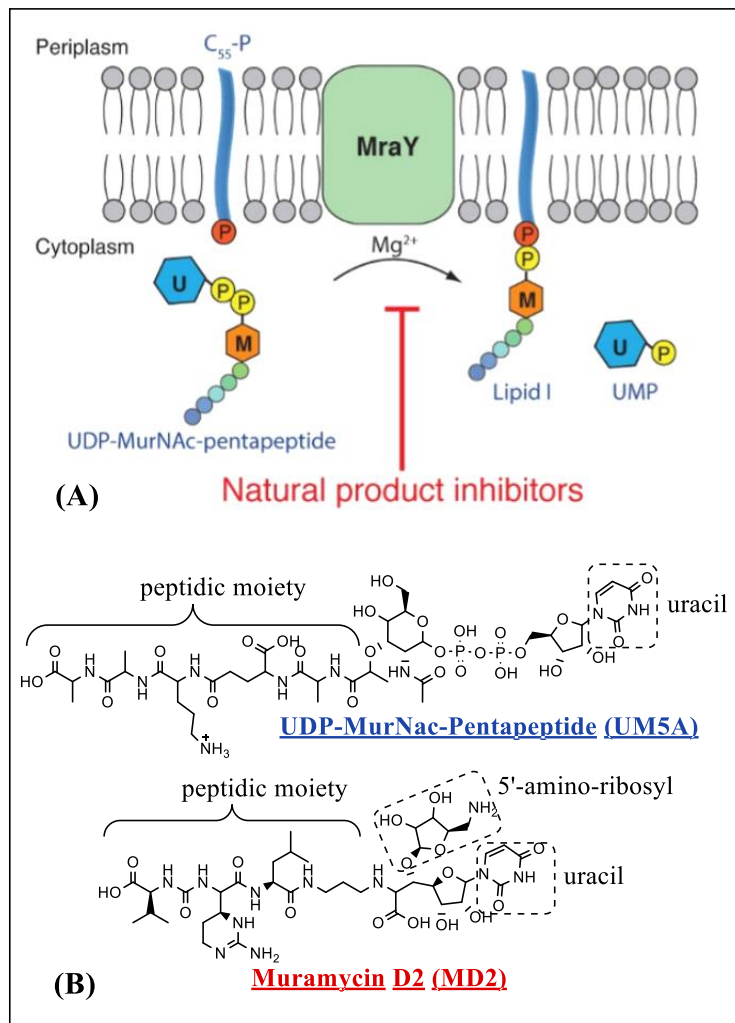


Figure 5: (A) *MraY* catalyzes the first reaction of peptidoglycan synthesis forming Lipid I. (B) UM5A is the natural substrate of *MraY*; MD2 is a natural inhibitor [4].

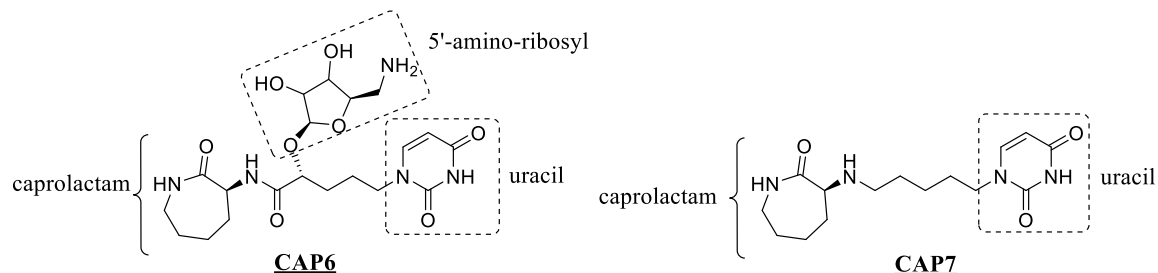
MurNac-pentapeptide (Figure 5B) carries the phospho-MurNac-pentapeptide group that is needed to form Lipid I, leaving uridine monophosphate as a byproduct after catalysis limited by magnesium. Muramycin D2 (MD2) seen in Figure 5B is a natural inhibitor

biosynthesis since the cell wall differentiates human and bacterial cells. *MraY* is the first integral membrane protein involved in biosynthesis of peptidoglycan and, as such, has great potential as a possible target for antitubercular drugs. Figure 5A shows how *MraY* catalyzes the synthesis of Lipid I to begin the process of making peptidoglycan- the

cross network of repeating sugar and amino acids. UDP-

of *MraY*. Recent cocrystal structures of *MraY* with UM5A and MD2 show the active site activity involved for each, confirming the importance of the uracil moiety and 5'-amino-ribose for inhibition of *MraY* [4]. While MD2 has proven its broad-spectrum antimicrobial activity, other natural inhibitors such as capuramycin which contains a caprolactam moiety have shown *Mtb*-specific inhibition [15]. Because the synthesis of natural inhibitors is very involved, and they have shown poor pharmacokinetic properties, there is a need for structure-based design and synthesis of narrow-spectrum antibiotics which target *MraY* of *Mtb*.

The following molecules in **Figure 6** were designed by Sudeshna Roy, PhD as potential inhibitors of *MraY*. CAP6 was designed with the uracil moiety and 5'-amino-



ribose moieties which were essential to MD2 inhibition of *MraY* as well as a caprolactam moiety which is found in the TB-specific natural inhibitor capuramycin. Before synthesis of CAP6 and CAP7 began, computational studies were done to show the potential binding in *MraY*. Because tunicamycin is a nucleoside antibiotic targeting *MraY*, the model used to dock the compounds was the tunicamycin-*MraY* co-crystal structure (5JNQ). These computational studies allowed for the comparison of CAP6 and CAP7 to known inhibitors, so that the efficacy of the new analogs could be predicted as shown in **Table 1**. The GlideScore gives insight into how well the molecule is expected to bind the enzyme; this value can be used to determine the binding free energy of the interaction. Because of this relationship, as the magnitude of a negative score increases,

the more favorable or spontaneous the binding is expected to be. The experimental reported activities are also given for the positive controls to give an idea of the possible

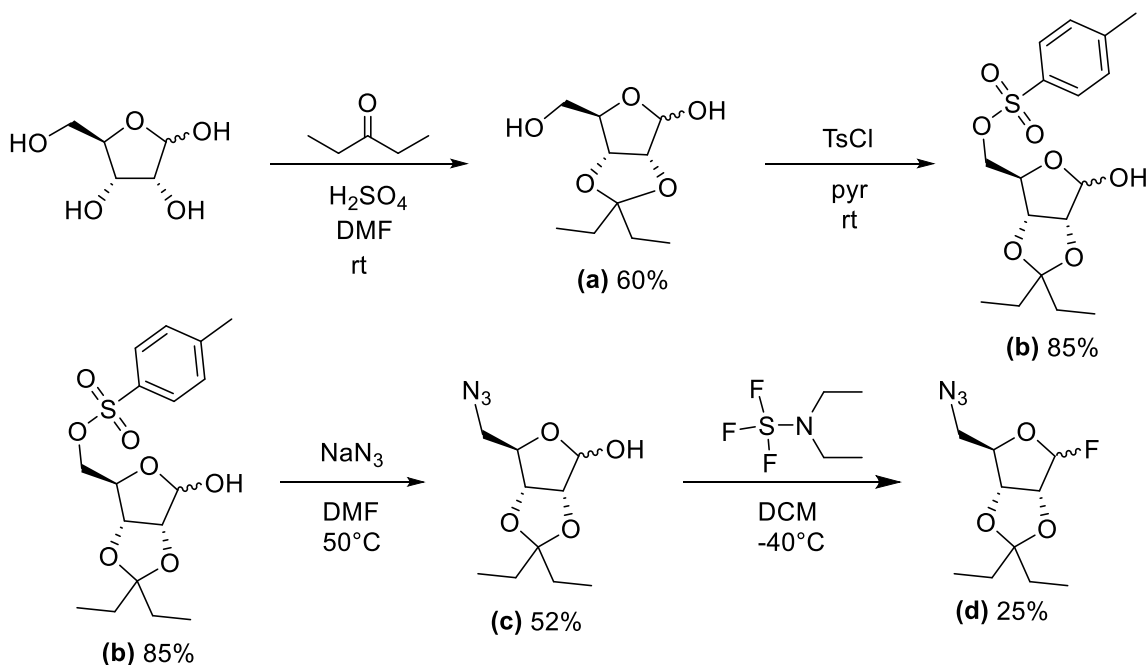
Compound		Experimental reported activity (μmol)	GlideScore (kcal/mol)	Binding Free-Energy (kcal/mol)
Positive Controls	Tunicamycin	$\text{IC}_{50} = 0.5-2.4$	-9.123	-71.269
	MuraymycinD2 (MD2)	$K_d = 0.014$	-8.882	-69.373
	5-aminoribosyl uridine	$K_d = 0.283$	-6.978	-54.248
	Capuramycin	$\text{IC}_{50} = 0.127$	-6.946	-67.428
Designed Compounds	CAP6	-	-8.184	-56.200
	CAP7	-	-8.334	-62.209

Table 1: The GlideScores and binding free energies were calculated through docking studies so that the binding of known inhibitors (positive controls) could be compared to the potential binding of CAP6 and CAP7. The designed analogs have scores falling within in the range of positive controls and as such are promising analogs.

value for CAP6 and CAP7. The studies showed that CAP6 and CAP7 had comparable GlideScores and Binding Free-Energies as other known inhibitors. This confirmed that CAP6 and CAP7 had great potential as antitubercular agents, so their syntheses became the goal of this project.

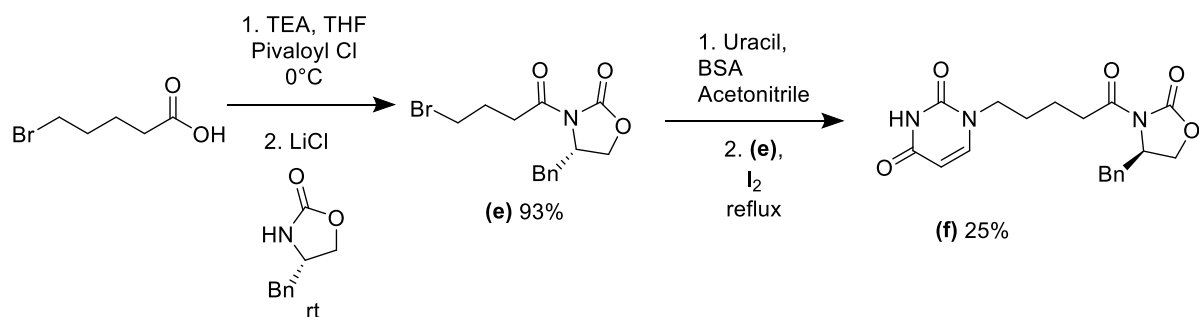
Section 2.2 – Results and discussion

CAP6 related reactions



Scheme 1: 5'-amino-ribosyl synthesis

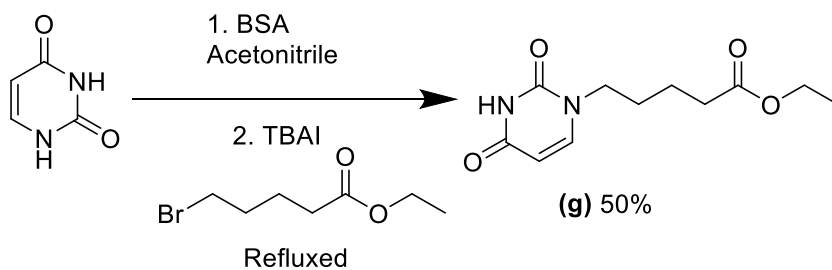
In order to prepare the 5'-amino-ribosyl for CAP6 as shown in **Scheme 1**, the 2' and 3' alcohols on the ribose sugar needed to be protected while leaving the other two alcohols available for the ensuing reactions. This was done by adding pentan-3-one and sulfuric acid in DMF to make the product **(a)** with 60% yield. To then improve the primary alcohol as a leaving group, a bulky tosyl group was added as tosyl chloride with the base pyridine producing product **(b)** with a yield of 85%. Sodium azide was then added to the solution of **(b)** in DMF to install the azide at the 5'-carbon. Because this moiety was being synthesized to be added to the main chain of CAP6, DAST was added to **(c)** in DCM to fluorinate the 1'-carbon. This produced the product **(d)** with a yield of 25% as a result of difficulty in purification; specifically, separation of the enantiomers through silica gel column proved difficult.



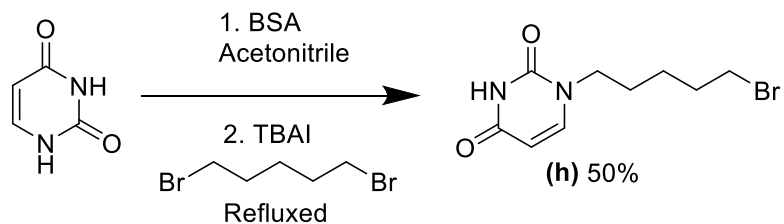
Scheme 2: Uracil attachment to the main chain

Scheme 2 shows the reactions used to prepare the main chain of CAP6 for the additions of 5'-amino-ribosyl and caprolactam. To begin this synthesis, a two-step reaction was used to install Evan's chiral auxiliary which would provide specificity of the enantiomer produced when caprolactam was added. The first step involved adding the base TEA and pivaloyl chloride in THF. This was followed by the addition of the auxiliary with LiCl and gave 93% yield. Following this reaction, BSA was added to a solution of uracil and acetonitrile. When the solution became clear, (e) and a catalytic amount of I₂ were added and refluxed to yield 25% of the product (f).

CAP7 related reactions

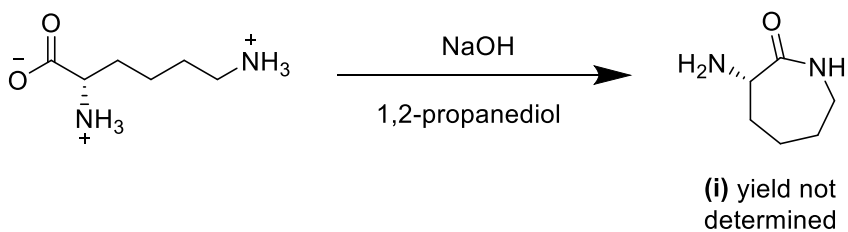


Reaction 1: Uracil attachment to ethyl 5-bromopentanoate



Reaction 2: Uracil attachment to 1,5-dibromopentane

In order to synthesize CAP7, uracil and caprolactam both needed to be added to a five-carbon chain. The uracil moiety was attached to the main chains in **Reactions 1** and **2**. For both reactions, uracil was added to BSA in acetonitrile. Once the solution became clear, a catalytic amount of TBAI and ethyl 5-dibromopentane and 1,5-dibromopentane were added and yielded 50% of **(g)** and **(h)** respectively. In both cases, a disubstituted product was formed leading to these yields. **Reaction 1** would have been followed by a reduction and bromination; rather than proceeding with these steps, **Reaction 2** provided a more effective option.



Reaction 3: Caprolactam synthesis

After uracil was added to the main chain for CAP7, caprolactam needed to be synthesized. This was done by cyclizing lysine. Before using propylene glycol, ethanol was used and produced no yield. While propylene glycol was more successful in cyclizing lysine, the difficulty in removing the solvent prevented the purification of the product **(i)** from being used. Attempts were made to distill propylene glycol out of the

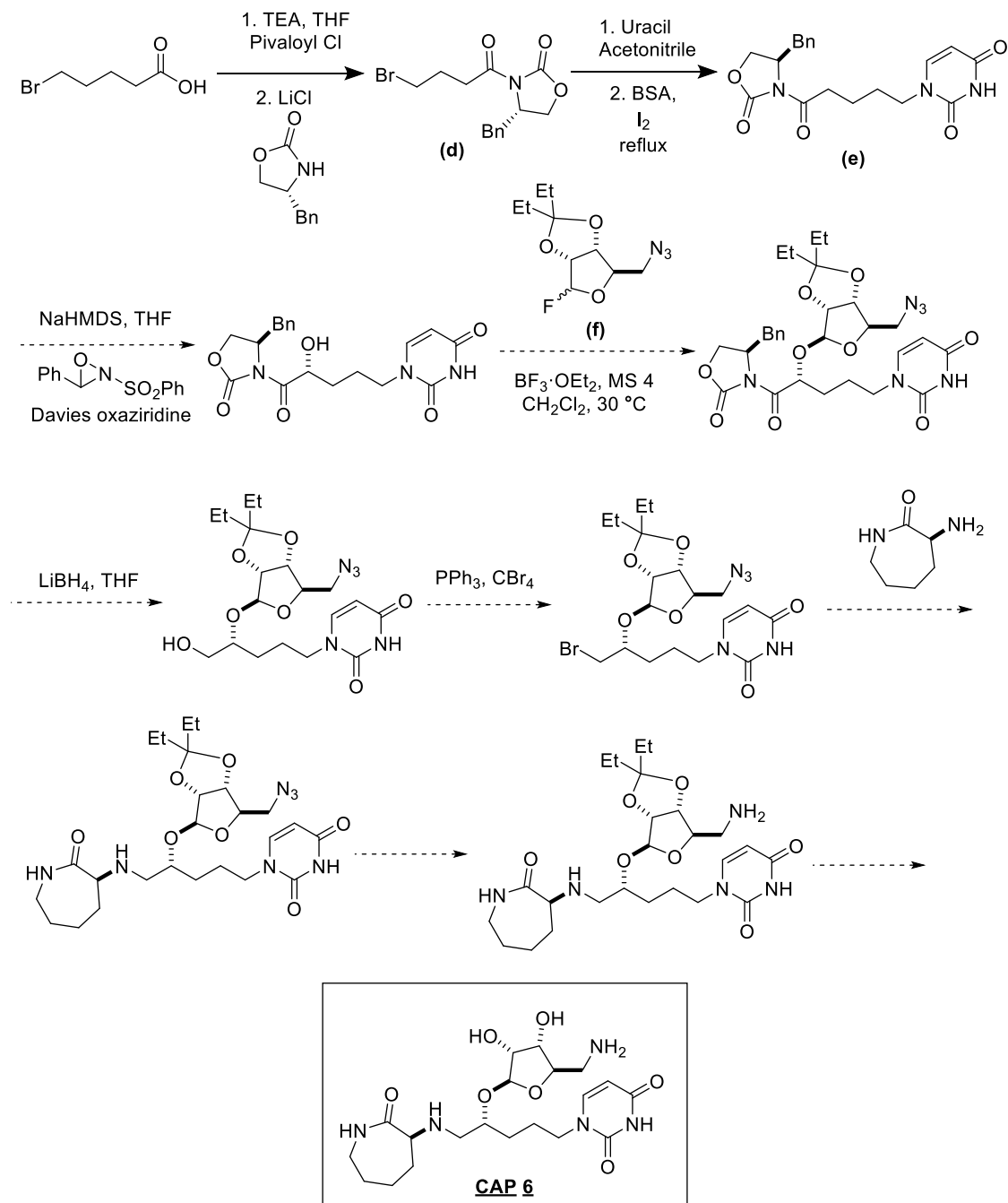
crude mixture; however, NMR showed that propylene glycol as well as lysine still remained.

Section 2.3 – Conclusion and future work

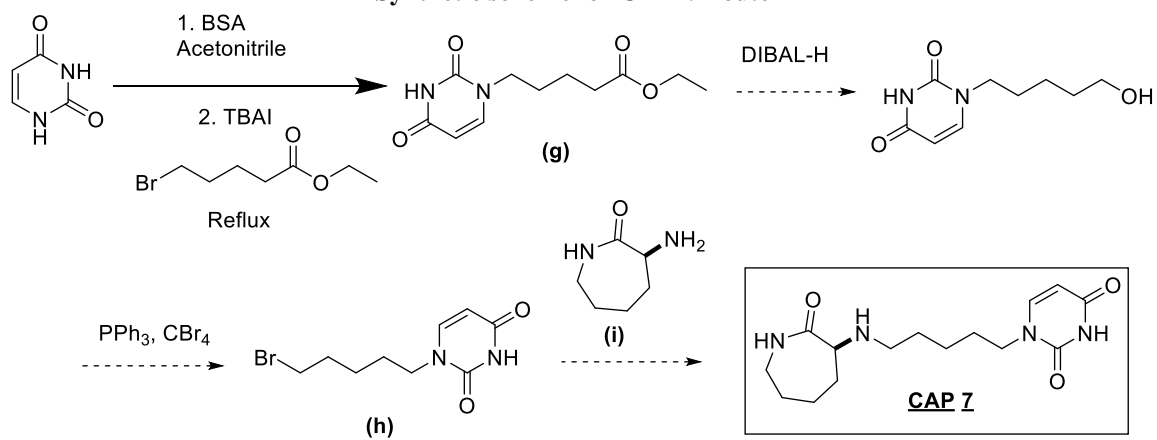
Though CAP6 and CAP7 were not completed during this project, the reactions completed contributed to the improvement of the synthetic routes for these analogs. Shamba Chaterjee, PhD and Tomayo Berida of Roy Laboratory have continued this project and found different synthetic routes for CAP6 and CAP7 and have tested these compounds. The initial testing of these compounds showed that they were not active against Mtb, but further testing will be done to determine if the compounds are active against other bacteria.

Section 2.4 – Characterization data and synthetic schemes

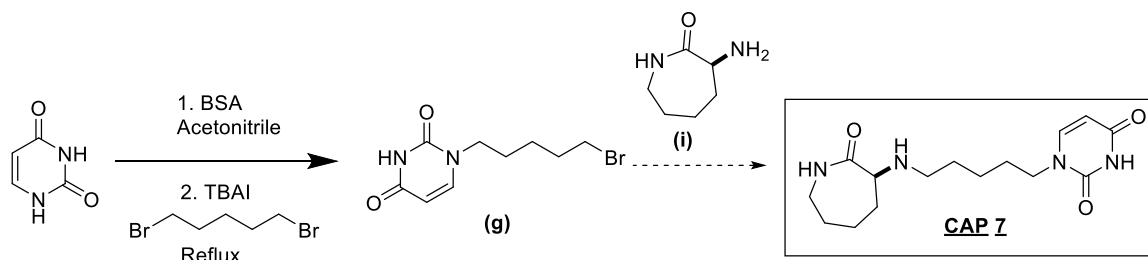
Synthetic scheme for CAP6



Synthetic scheme for CAP7: Route 1

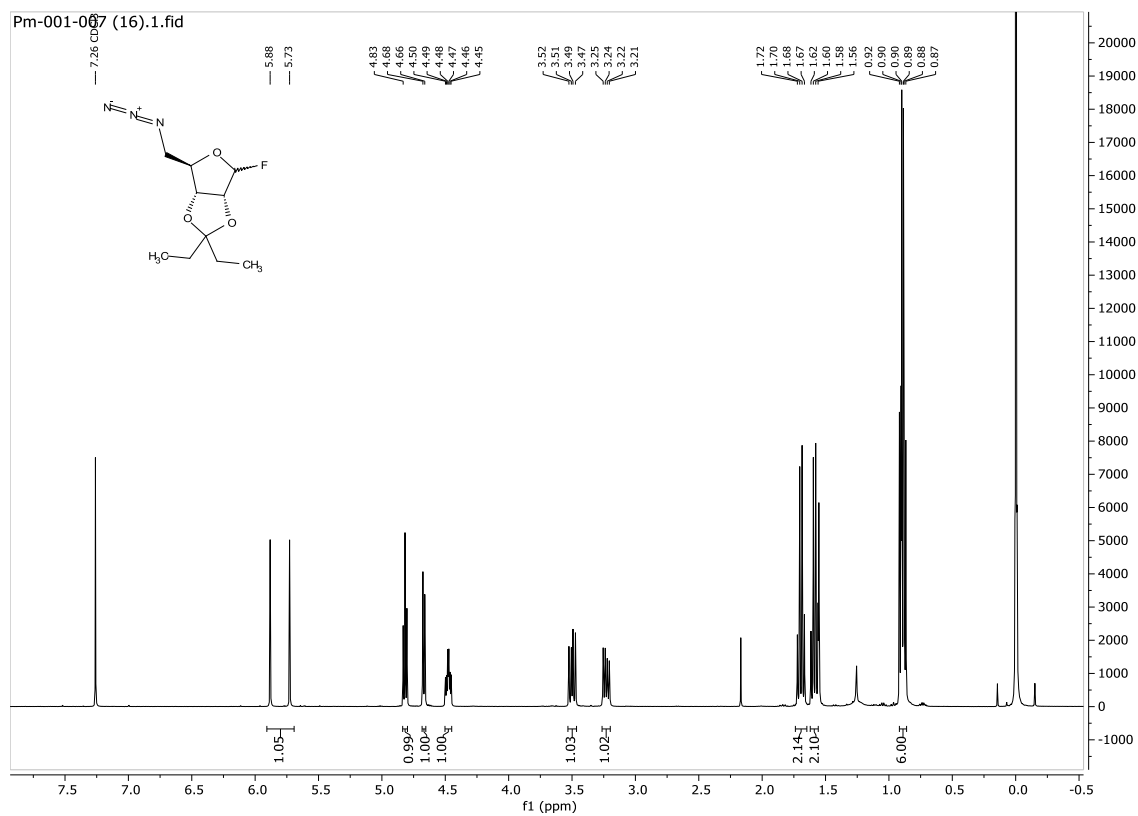


Synthetic scheme for CAP7: Route 2

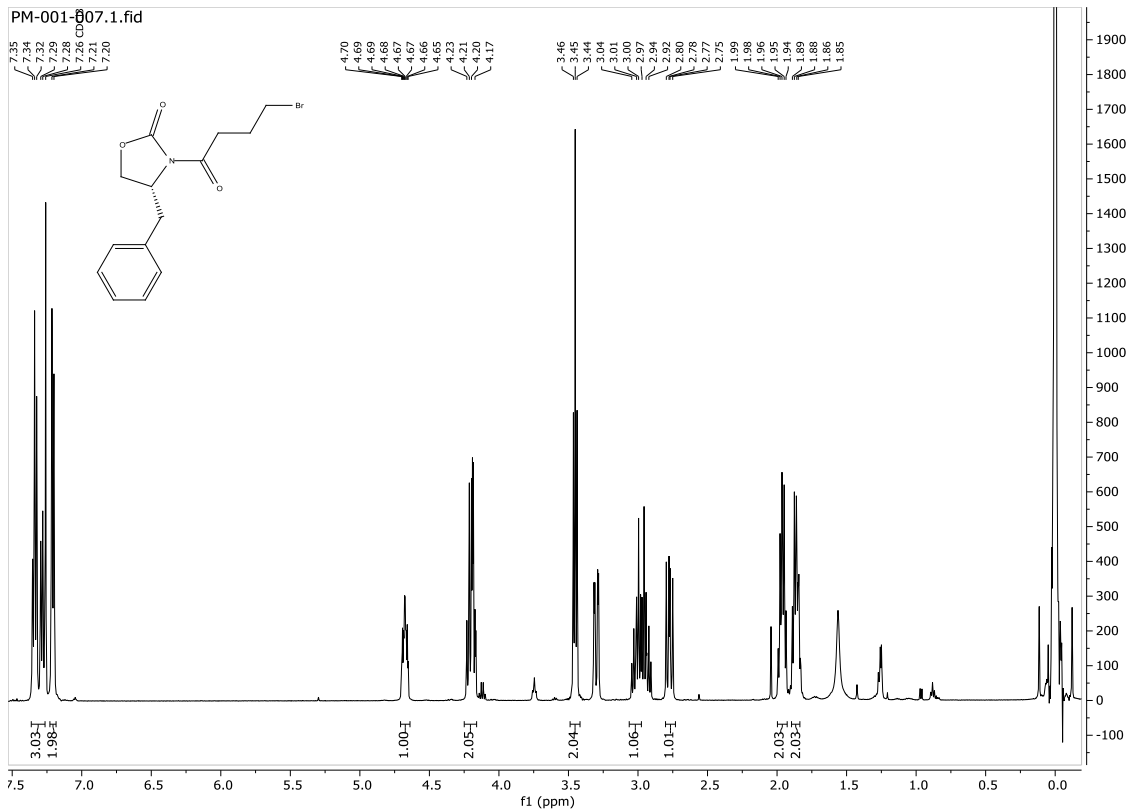


(3aR,4R,6aR)-4-(azidomethyl)-2,2-diethyl-6-fluorotetrahydrofuro[3,4-d][1,3]dioxole

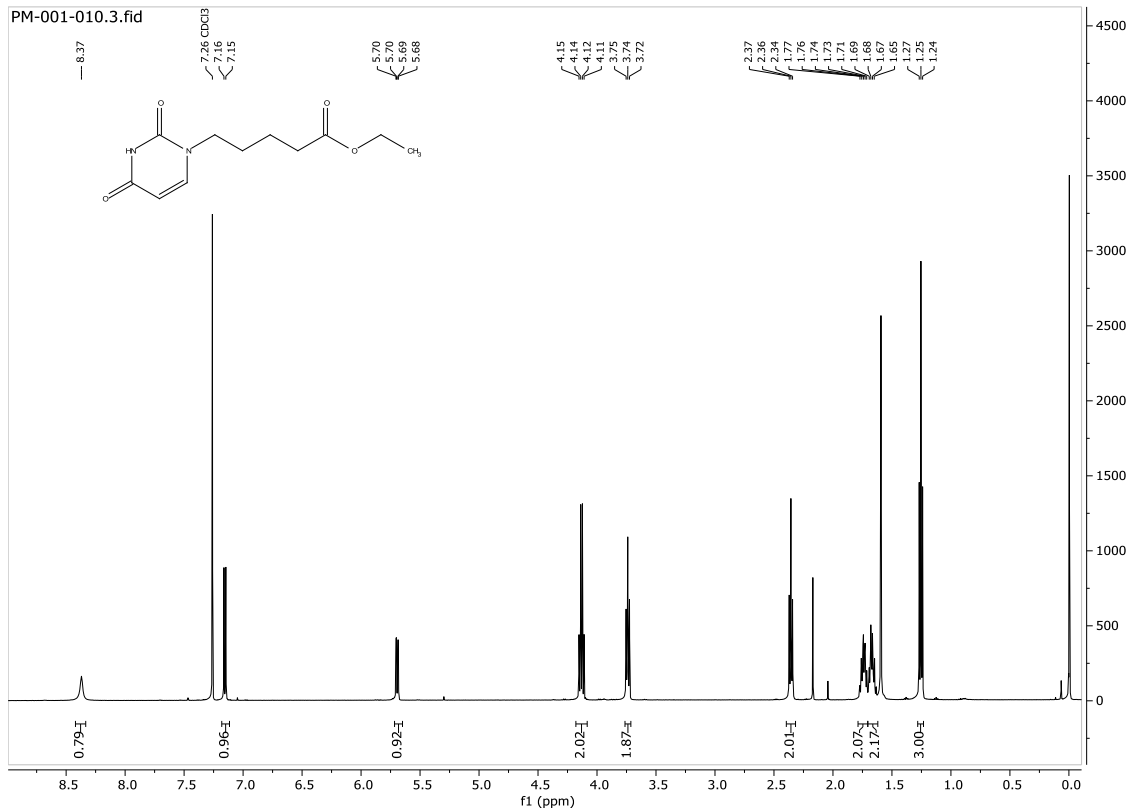
(d)



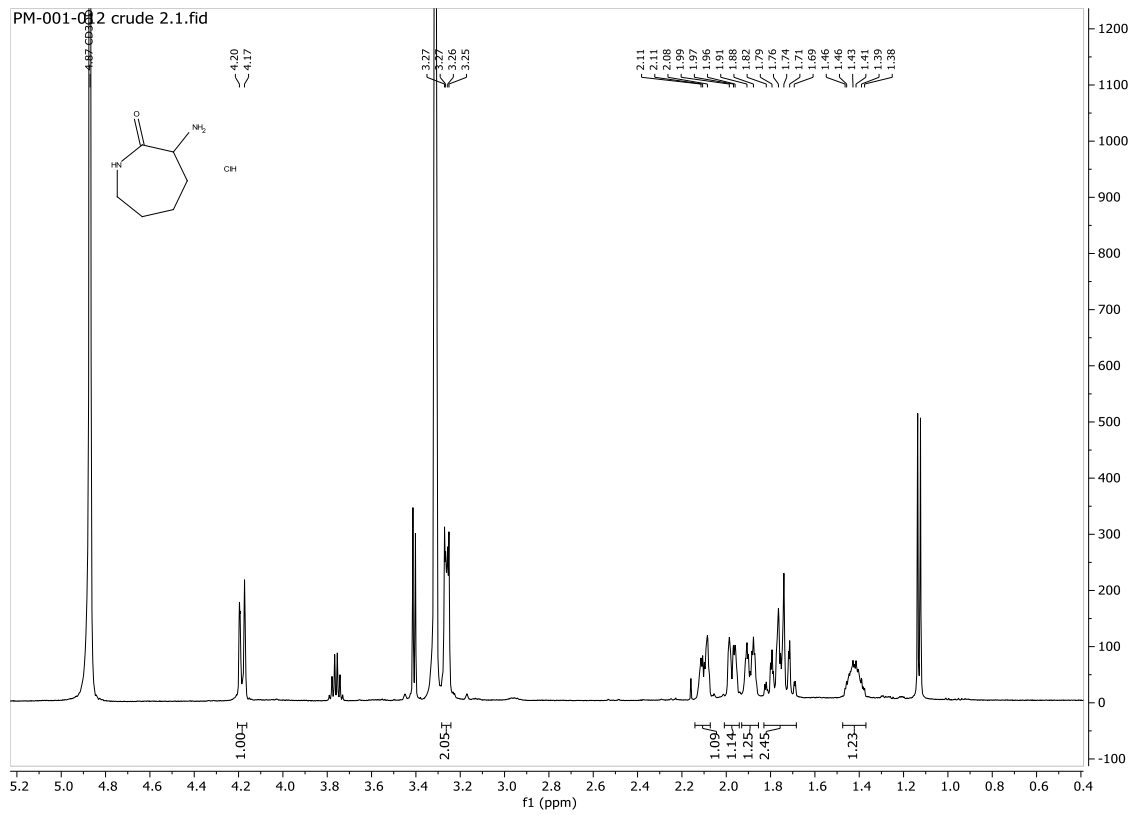
(R)-4-benzyl-3-(4-bromobutanoyl) oxazolidin-2-one (e)



Ethyl 5-(2,4-dioxo-3,4-dihydropyrimidin-1(2H)-yl) pentanoate (g)



(S)-3-aminoazepan-2-one (i)

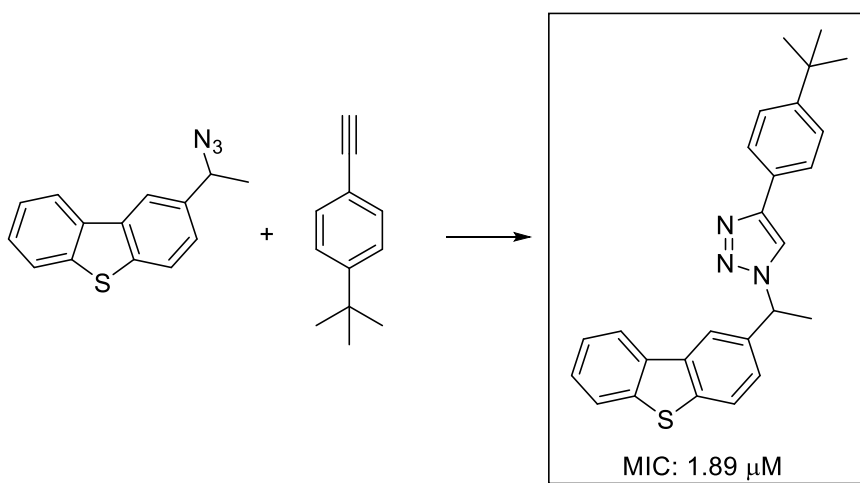


Chapter 3: Fluorinated triazoles in antitubercular analogs

Section 3.1 – Literature precedent and proposed project

Previous research has shown that carbazoles and dibenzofurans which exist in natural antitubercular analogs play vital roles in their activity. Additionally, 1,2,3-triazoles have been shown to have antitubercular activity when conjugated with heterocyclic moieties. Based on these findings, Patpi used a molecular hybridization approach of combining carbazole, dibenzofuran, and dibenzothiophene moieties with a variety of substituted 1,2,3-triazoles to test their efficacy as antitubercular agents. Their synthetic route consisted of synthesis of azides on the carbazoles, dibenzofurans, and dibenzothiophene moieties which were then coupled with various substituted alkynes through Huisgen cycloadditions to produce the analogs for testing against Mtb. The assays used on strain H37Rv of Mtb showed that dibenzothiophene-containing analogs had the lowest Minimum Inhibitory Concentration (MIC) values which are the lowest values at which the compounds inhibited visible growth of Mtb and, therefore, are preferable when smaller values. Patpi's analog shown below has an MIC value of 1.89

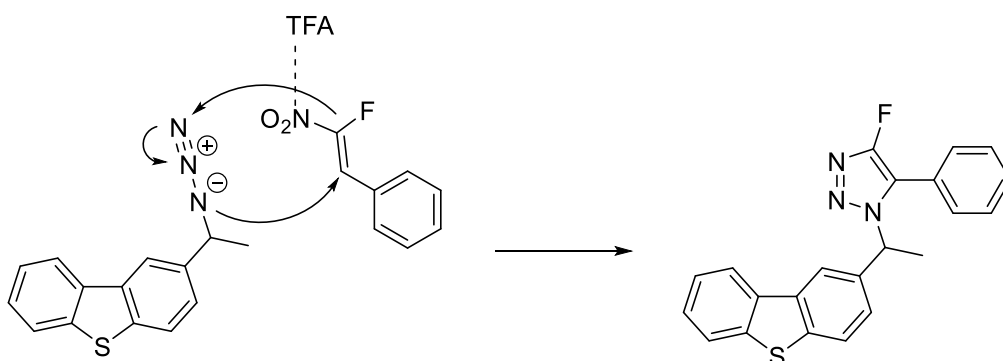
Huisgen cycloaddition ("Click" Chemistry)



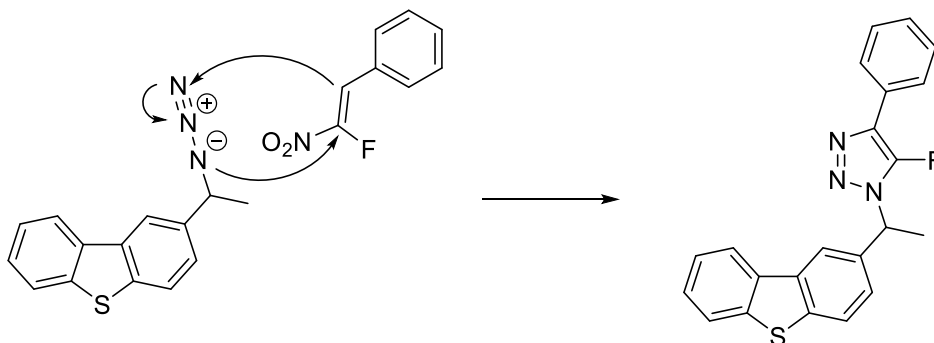
μM which is considerably lower than that of pyrazinamide (50.08 μM) and ethambutol (7.6 μM) but higher

than that of isoniazid (0.37 μM). [5]

This compound provided a starting point for this project. By using a cyclization technique developed by Roy lab, a fluorinated version of this analog could be synthesized. Once synthesized, the effect of fluorine on the efficacy of the analog could be determined through antimicrobial assays. Because of fluorine's unique properties and ability of the C-F bond to act as a bio-isostere of the C-H bond, it was hypothesized that the addition of fluorine would increase the efficacy of the analog.



Mechanism 1 leading to 4-fluoro-1,5-substituted product

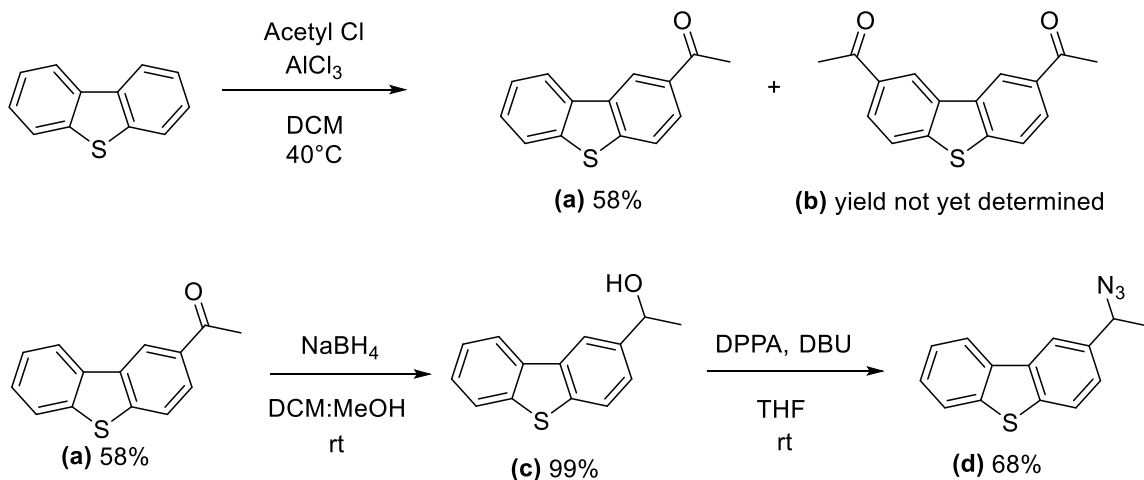


Mechanism 2 leading to 5-fluoro-1,4-substituted byproduct with no TFA

Mechanism 1 above was proposed by Roy lab for the synthesis of 4-fluoro, 1,5-substituted triazoles. Trifluoroacetic acid coordinates with the nitro group to further activate it as an electron withdrawing group, making the adjacent carbon act as a nucleophile and the benzylic carbon act as an electrophile affording the cyclization as shown. When TFA was not used, it was found that a mixture of 4-fluoro, 1,5-substituted

product and 5-fluoro, 1,4-substituted byproduct in a ratio of 5:2 was produced. Though the aim of Roy lab was to find a method of producing one regioselective isomer, the latter reaction which produces both isomers would be more useful for this product because the analogs of interest which were synthesized by Patpi were 1,4-substituted-1,2,3-triazoles.

Section 3.2 – Results and Discussion

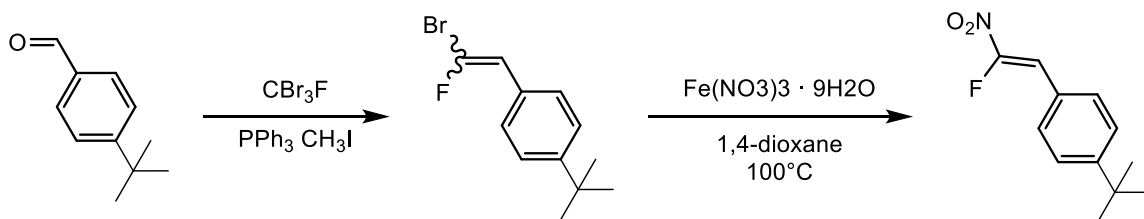


Synthetic scheme for azide synthesis

Because dibenzothiophene was commercially available and more affordable than the acylated dibenzothiophene, it was the starting point for the synthesis of the azide (**d**). Friedel-Crafts acylation was used to obtain product (**a**) with a 58% yield; this yield was primarily a result of the production of the diacetylated byproduct (**b**) which made separation through silica gel column difficult. Sodium borohydride reduction was then used to reduce the newly installed acetyl group to an alcohol (**c**) and produced practically stoichiometric yields. From the alcohol in (**c**), the azide (**d**) was produced by adding diphenylphosphoryl azide (DPPA) and the base 1,8-Diazabicyclo[5.4.0]undec-7-ene (DBU) giving 68% yield of the product (**d**).

Section 3.3 – Conclusion and Future Work

As a result of the COVID-19 pandemic, this project was not able to be completed. Given more time, the fluoro-nitro compounds would have been synthesized so that the cyclization leading to the final analog could be completed. Since the azide was already synthesized, a variety of different fluoro-nitro compounds could be synthesized and cyclized to form the 1,2,3-triazole. The synthesis of the fluoro-nitro compounds would have been done by adding CBr_3F , PPh_3 , and CH_3I to react with the aldehyde seen in scheme below. At the same time, the original non-fluorinated compounds would have been synthesized through Huisgen cycloaddition. Once the fluorinated and non-fluorinated compounds were completed, they would have been tested on antimicrobial assays to determine their efficacy. With the assistance of a collaborating lab, the compounds would have been assayed against Mtb.

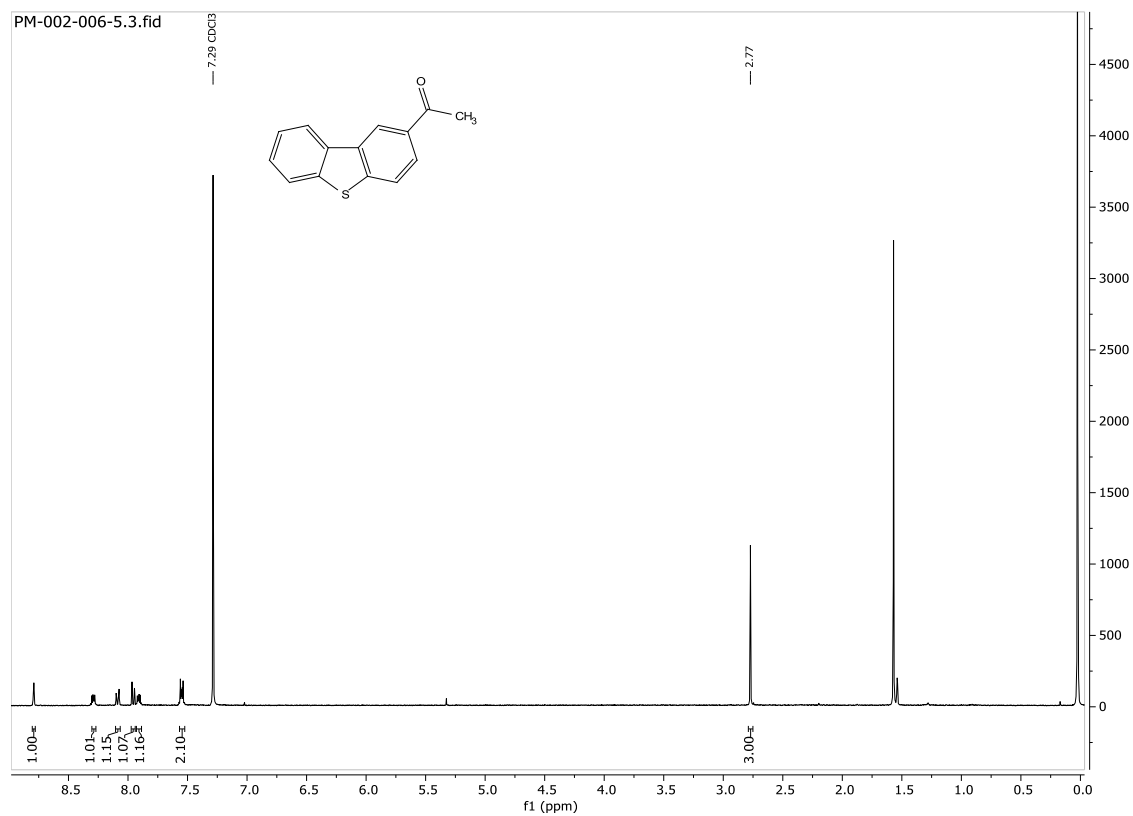


Synthetic scheme for fluoro-nitro synthesis

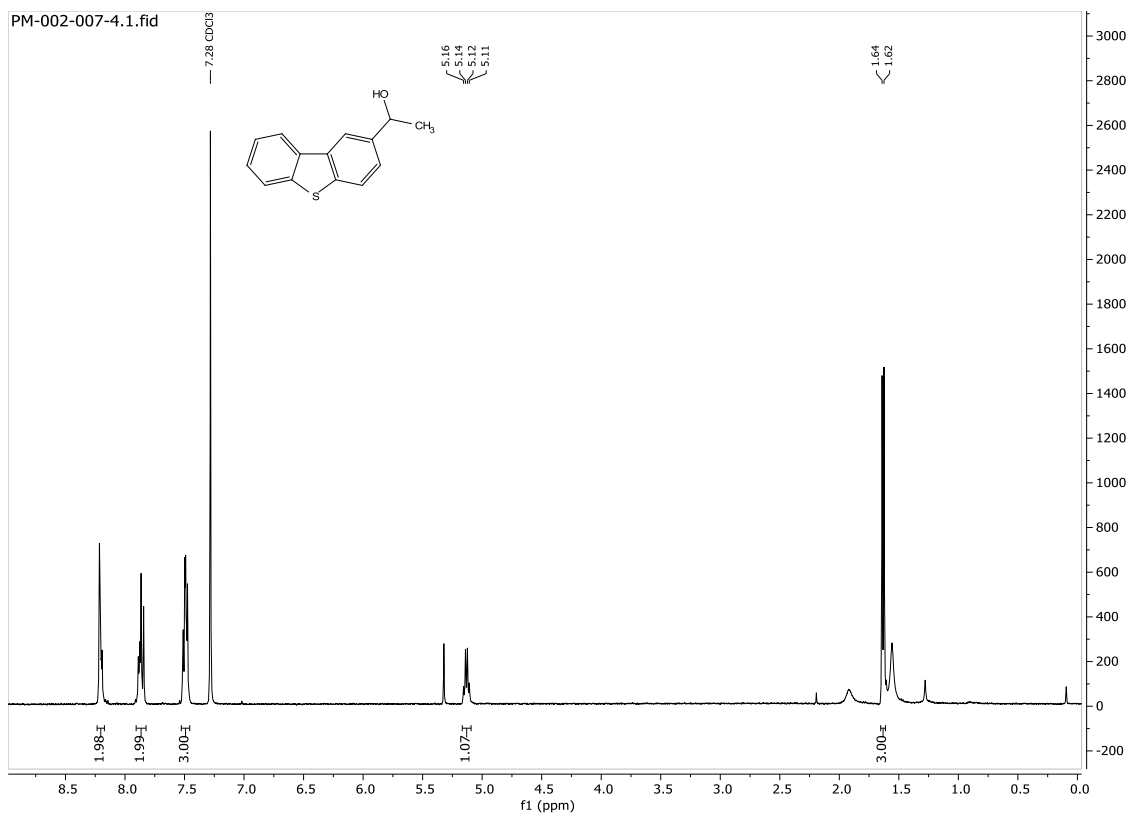
Though the pandemic of COVID-19 currently affecting the entire world is an urgent matter and demands the cooperation of all individuals to slow its spread, the same is true of TB. Diseases are forever evolving, and while research now moves faster than ever towards new/repurposed drugs and vaccines to face them, TB has been the exception for far too long. Though the lab is not currently accessible, this project will be continued by gathering information for reviews to aid other researchers as well as by spreading awareness of this disease.

Section 3.4 – Characterization data (H^1 NMR)

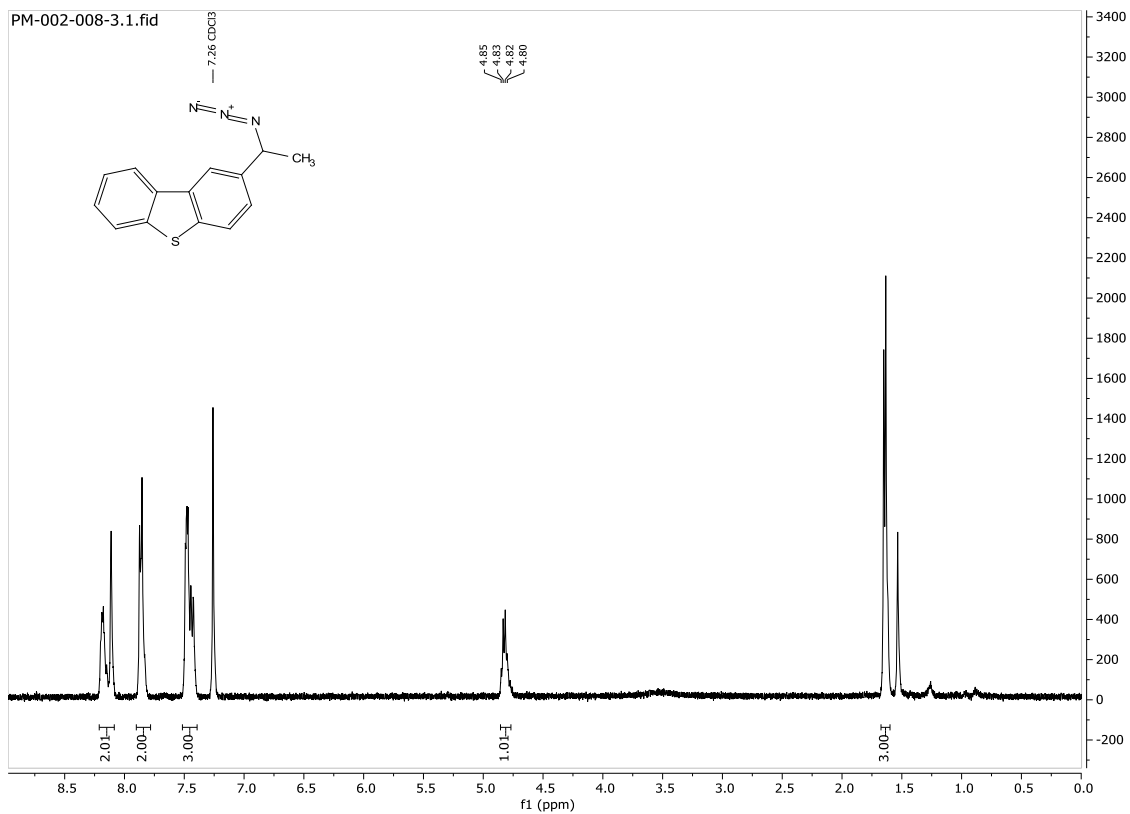
1-(dibenzo[b,d]thiophen-2-yl)ethan-1-one (a)



1-(dibenzo[b,d]thiophen-2-yl)ethan-1-ol (c)



2-(1-azidoethyl)dibenzo[b,d]thiophene (d)



Chapter 4: Supplemental Information

Section 4.1 – References

- [1] C. Nunes-Alves, M. G. Booty, S. M. Carpenter, P. Jayaraman, A. C. Rothchild and S. M. Behar, "In search of a new paradigm for protective immunity to TB," *Nature Reviews Microbiology*, vol. 12, pp. 289-299, 2014.
- [2] P. Nahid, S. Dorman, N. Alipanah, P. Barry, J. Brozek and A. Cattamanchi, "Executive Summary: Official American Thoracic Society/Centers for Disease Control and Prevention/Infectious Diseases Society of America Clinical Practice Guidelines: Treatment of Drug-Susceptible Tuberculosis," *Clinical Infectious Diseases*, vol. 63, no. 7, pp. 853-867, 2016.
- [3] Global Tuberculosis Report 2019, France: World Health Organization 2019, 2019.
- [4] B. C. Chung, E. H. Mashalidis, T. Tanino, M. Kim, A. Matsuda, J. Hong, S. Ichikawa and S. Yong Lee, "Structural insights into inhibition of lipid I," *Nature*, vol. 533, pp. 557-559, 2016.
- [5] S. R. Patpi, L. Pulipati, P. Yogeewari, D. Sriram, N. Jain, B. Sridhar, R. Murthy, A. D. T, S. V. Kalivendi and S. Kantevari, "Design, Synthesis, and Structure–Activity Correlations of Novel Dibenzo[b,d]furan, Dibenzo[b,d]thiophene, and N-Methylcarbazole," *Journal of Medicinal Chemistry*, vol. 55, no. 8, pp. 3911-3922, 2012.
- [6] I. Barberis, N. L. Bragazzi, L. Galluzzo and M. Martini, "The history of tuberculosis: from the first historical records to the isolation of Koch's bacillus," vol. 58, no. 1, 2017.
- [7] Division of Tuberculosis Elimination, "Centers for Disease Control and Prevention," October 2011. [Online]. Available: <https://www.cdc.gov/tb/publications/factsheets/general/tb.htm>. [Accessed 13 April 2020].
- [8] J. W. Bartholomew and T. Mittwer, "The Gram Stain," *American Society for Microbiology: Bacteriology Reviews*, vol. 16, no. 1, pp. 1-29, 1952.
- [9] L. J. Alderwick, J. Harrison, G. S. Lloyd and H. L. Birch, "The Mycobacterial Cell Wall–Peptidoglycan and Arabinogalactan," *Cold Springs Harbor Perspectives in Medicine*, vol. 5, no. 8, pp. 1-15, 2015.
- [10] K. Gould, "Antibiotics: from prehistory to present day," no. 71, 2016.
- [11] D. E. Goldberg, R. F. Siliciano and W. R. Jacobs, "Outwitting Evolution: Fighting Drug-Resistant TB, Malaria, and HIV," *Cell*, pp. 1271-1283, 2012.

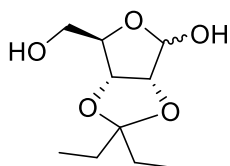
- [12] P. Gopal, J. Sarathy, M. Yee, P. Ragunathan, J. Shin, S. Bhushan and J. Zhu, "Pyrazinamide triggers degradation of its target aspartate decarboxylase," *Nature Communication*, vol. 11, no. 1661, pp. 1-10, 2020.
- [13] T. Oettinger, M. Jorgensen, A. Ladefoged, K. Haslov and P. Andersen, "Development of the Mycobacterium bovis BCG vaccine: review of the historical and biochemical evidence for a genealogical tree," *Tubercle and Lung Disease*, vol. 79, no. 4, pp. 243-250, 1999.
- [14] A. Zwerling, M. A. Behr, A. Verma, T. F. Brewer, D. Menzies and M. Pai, "The BCG World Atlas: A Database of Global BCG Vaccination Policies and Practices," *PLoS Medicine*, vol. 8, no. 3, 2011.
- [15] M. Winn, R. J. M. Goss, K. Kimura and T. Bugg, "Antimicrobial nucleoside antibiotics targeting cell wall assembly: Recent advances in structure-function studies and nucleoside biosynthesis.," *Natural Products Reports*, vol. 27, no. 2, pp. 279-304, 2010.
- [16] S. Jana, S. Adhikari, M. R. Cox and S. Roy, "Regioselective synthesis of 4-fluoro-1,5-disubstituted-1,2,3-triazoles from synthetic surrogates of α -fluoroalkynes," *Chemical Communications*, vol. 56, no. 12, pp. 1871-1874, 2020.
- [17] Y. Ma, C. R. Horsburgh, L. F. White and H. E. Jenkins, "Quantifying TB transmission: a systematic review of reproduction number and serial interval estimates for tuberculosis," *Epidemiology and Infection*, vol. 146, no. 12, 2018.

Section 4.2 – Synthetic procedures for Chapter 2

CAP6 experimental procedures

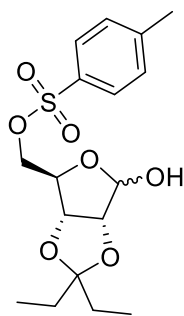
(3aR,6R,6aR)-2,2-diethyl-6-(hydroxymethyl) tetrahydrofuro[3,4-d][1,3]dioxol-4-ol

(a)



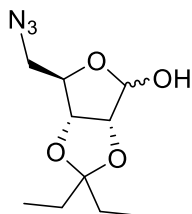
Dry DMF (15 mL) was added to (3R,4S,5R)-5-(hydroxymethyl)tetrahydrofuran-2,3,4-triol (1.0 g, 1 Eq, 6.7 mmol), then treated with pentan-3-one (29 g, 35 mL, 50 Eq, 0.33 mol) and sulfuric acid (0.65 g, 1 Eq, 6.7 mmol) in a round-bottom flask. The mixture was stirred at room temperature for 45 hours and yielded 850 mg (58% yield) of a colorless syrup.

(3aR,4R,6aR)-2,2-diethyl-6-hydroxytetrahydrofuro[3,4-d][1,3]dioxol-4-yl)methyl 4-methylbenzenesulfonate (b)



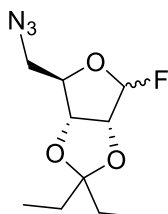
At 0°C, to a solution of protected D-ribose (1.1 g, 5.0 mmol) in pyridine (15 mL) was added recrystallized tosyl chloride (1.4 g, 7.6 mmol). The mixture was stirred at rt for 17 h. After completion of the reaction, the reaction was quenched with water and EtOAc was added. The resulting solution was transferred into a separatory funnel and washed with a 1 M HCl aqueous solution. The organic layer was washed with brine and water, dried (Na₂SO₄), filtrated and concentrated in vacuo giving 85% yield of the crude tosylate **(b)** as a translucent bright orange oil. This residue was used for the following azidation reaction.

(3aR,6R,6aR)-6-(azidomethyl)-2,2-diethyltetrahydrofuro[3,4-d][1,3]dioxol-4-ol (c)



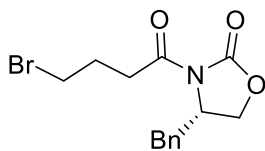
Sodium azide (0.65 g, 10 mmol) was added to the protected ribose (1.6 g, 4.3 mmol) and DMF (15mL) was added to the solution in a round-bottom flask. The mixture stirred at 50°C for 18h and yielded 0.54 g (52% yield) of **(c)**. ¹H NMR (400 MHz, Chloroform-*d*) δ 5.52 (d, *J* = 5.2 Hz, 1H), 4.74 – 4.67 (m, 2H), 4.47 – 4.35 (m, 1H), 3.63 (dd, *J* = 12.6, 7.0 Hz, 1H), 3.45 (dd, *J* = 12.6, 5.6 Hz, 1H), 3.10 (d, *J* = 5.2 Hz, 1H), 1.83 – 1.69 (m, 2H), 1.69 – 1.56 (m, 3H), 0.95 (dt, *J* = 14.7, 7.4 Hz, 6H).

(3aR,4R,6aR)-4-(azidomethyl)-2,2-diethyl-6-fluorotetrahydrofuro[3,4-d][1,3]dioxole (d)



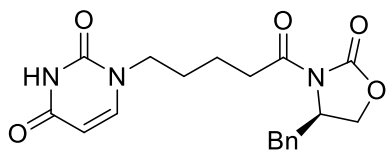
A solution of **(c)** was treated with DAST at -40°C for 30 minutes. The reaction was quenched by addition of aqueous NaHCO₃ after the TLC showed there was no remaining starting material. Then, the organic phase was dissolved in diethyl ether, washed with H₂O and saturated aqueous NaCl, dried (Na₂SO₄), filtered, and concentrated in vacuo. A column was run from 0-40% EA-Hex. The crude product was a slightly yellow liquid. The four spots were not completely separated by the column leading to the 25% yield of **(d)**. ¹H NMR (400 MHz, Chloroform-*d*) δ 5.80 (d, *J* = 61.3 Hz, 1H), 4.82 (t, *J* = 5.9 Hz, 1H), 4.67 (dd, *J* = 6.0, 1.0 Hz, 1H), 4.48 (dddd, *J* = 7.6, 6.5, 3.5, 0.9 Hz, 1H), 3.50 (dd, *J* = 12.9, 7.7 Hz, 1H), 3.25 (d, *J* = 6.6 Hz, 1H), 1.69 (q, *J* = 7.4 Hz, 2H), 1.59 (q, *J* = 7.5 Hz, 2H), 0.89 (td, *J* = 7.5, 5.3 Hz, 6H).

(R)-4-benzyl-3-(4-bromobutanoyl) oxazolidin-2-one (e)



A stirred solution of 5-bromopentanoic acid (500 mg, 1 Eq, 2.76 mmol) in dry THF (5 mL) at 0 °C was treated with triethylamine (699 mg, 0.96 mL, 2.5 Eq, 6.90 mmol) and pivaloyl chloride (366 mg, 0.37 mL, 1.1 Eq, 3.04 mmol). The viscous suspension was stirred for 1 h. Then, lithium chloride (129 mg, 1.1 Eq, 3.04 mmol) and (R)-4-benzyl-2-oxazolidinone (245 mg, 1.38 mmol, 1.00 eq.) were added. The suspension was stirred at the same temperature for 0.5 h and then warmed to room temperature and stirred for another 3 h. Next, water (5 mL) was added and the solution was concentrated under reduced pressure. The aqueous phase was extracted three times with EtOAc (25 mL per extraction). The combined organic phases were dried (Na₂SO₄), the volatiles were evaporated under reduced pressure and the remaining oil was filtered through silica gel. The experiment yielded 840 mg (93.2% yield) of (e). ¹HNMR (500 MHz, Chloroform-d) δ 7.37 – 7.25 (m, 3H), 7.24 – 7.19 (m, 2H), 4.68 (ddt, J = 10.5, 7.2, 3.2 Hz, 1H), 4.25 – 4.16 (m, 2H), 3.45 (t, J = 6.6 Hz, 2H), 3.30 (dd, J = 13.4, 3.4 Hz, 1H), 2.98 (qt, J = 17.2, 7.2 Hz, 2H), 2.78 (dd, J = 13.3, 9.6 Hz, 1H), 2.03 – 1.79 (m, 4H).

(R)-1-(5-(4-benzyl-2-oxooxazolidin-3-yl)-5-oxopentyl) pyrimidine-2,4(1H,3H)-dione (f)

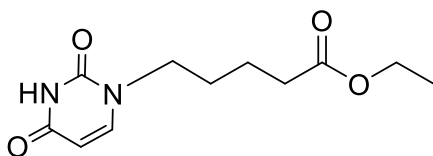


To a suspension of Uracil (100 mg) in dry acetonitrile (32 mL) was added trimethylsilyl N-(trimethylsilyl) acetimidate (448 mg, 541 μL, 2.5 Eq, 2.20 mmol) under argon. After the reaction mixture became a clear solution (half an hour), (e) (300 mg, 1

Eq, 882 μmol) and a catalytic amount of iodine (11.2 mg, 0.05 Eq, 44.1 μmol) were added. The reaction solution was heated at reflux for 72 h to yield a brown colored solution. Monitoring the reaction by TLC showed unreacted uracil and bromo-oxazolidinone. After cooling to room temperature, the mixture was quenched with water, diluted with ethyl acetate. Precipitation was observed. The organic layer was removed, and the aqueous layer was washed with EtOAc. The combined organic layer was washed with water, brine and dried over Na_2SO_4 and evaporated to dryness. The residue was purified by flash chromatography (40-100% EtOAc in hexane as eluent) to give (**f**) as a white foamy compound with 25% yield.

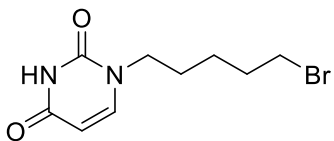
CAP7 experimental procedures

Ethyl 5-(2,4-dioxo-3,4-dihydropyrimidin-1(2H)-yl) pentanoate (g)



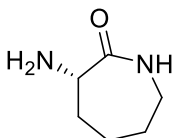
To a suspension of Uracil (281 mg) in dry acetonitrile (32 mL) was added trimethylsilyl N-(trimethylsilyl) acetimidate (2.27 g, 2.74 mL, 2.5 Eq, 11.2 mmol) under argon. After the reaction mixture became a clear solution (half an hour), ethyl 5-bromopentanoate (2.80 g, 2.12 mL, 3 Eq, 13.4 mmol) and a catalytic amount of TBAI (165 mg, 0.1 Eq, 446 μmol) were added. The reaction solution was heated at reflux for 3 days. The reaction was quenched by adding water dropwise and was worked up in ethyl acetate. The reaction yielded 51% yield of the product (**g**). ^1H NMR (500 MHz, Chloroform-*d*) δ 8.37 (s, 1H), 7.15 (d, $J = 7.9$ Hz, 1H), 5.69 (dd, $J = 7.9, 2.3$ Hz, 1H), 4.13 (q, $J = 7.1$ Hz, 2H), 3.74 (t, $J = 7.1$ Hz, 2H), 2.36 (t, $J = 7.1$ Hz, 2H), 1.80 – 1.70 (m, 2H), 1.70 – 1.63 (m, 2H), 1.25 (t, $J = 7.1$ Hz, 3H).

1-(5-bromopentyl) pyrimidine-2,4(1H,3H)-dione (h)



To a suspension of Uracil (1 g) in dry acetonitrile (15 mL) was added trimethylsilyl N-(trimethylsilyl) acetimidate (2 g, 1 Eq, 9 mmol) under argon. After the reaction mixture became a clear solution (half an hour), 1,5-dibromopentane (5 g, 3 mL, 2 Eq, 0.02 mol) and a catalytic amount of tetrabutylammonium iodide (3 g, 1 Eq, 9 mmol) were added. The reaction solution was heated at reflux for 3 days. The reaction was run in a vial and the white inner circle of the lid could not withstand the heat of the reaction and fell into the mixture. The lid was replaced after the first day of running and TLC showing the reaction was not complete. The white substance kept the stir bar from being able to stir. After 3 days, and the addition of a second equivalent of 1,5-dibromopentane (5 g, 3 mL, 2 Eq, 0.02 mol), the TLC still showed starting material, but the reaction was stopped. The reaction was quenched by adding water drop-wise and was worked up in ethyl acetate and yielded 50% (g).

(S)-3-aminoazepan-2-one (i)

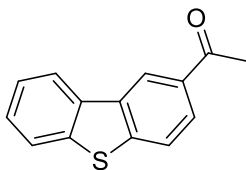


(S)-2,6-diammoniohexanoate (500 mg, 1 Eq, 3.40 mmol) was neutralized by sodium hydroxide (136 mg, 1 Eq, 3.40 mmol), then about 25 mL of propylene glycol was added to the round bottom flask. A dean stark trap was used to collect any water produced by the reaction. The mixture was heated to 200°C and allowed to reflux for 2 hours. The reaction mixture was distilled to remove propylene glycol which led to charring of the product before all of the propylene glycol could be removed. Because the propylene glycol could not be removed, the yield was not

determined. A crude NMR confirmed the formation of caprolactam. ^1H NMR (500 MHz, Methanol- d_4) δ 4.21 – 4.16 (m, 1H), 3.28 – 3.21 (m, 2H), 2.13 – 2.06 (m, 1H), 2.00 – 1.94 (m, 1H), 1.93 – 1.85 (m, 1H), 1.83 – 1.68 (m, 2H), 1.47 – 1.38 (m, 1H).

Chapter 3 Reactions

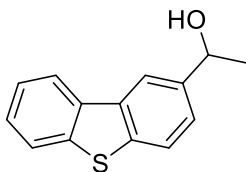
1-(dibenzo[b,d]thiophen-2-yl)ethan-1-one (a)



Aluminum chloride (0.80 g, 1.1 Eq, 6.0 mmol) was first measured out in a vial and flushed with argon. To this vial was added DCM (5 mL), then acetyl chloride (0.85 g, 0.77 mL, 2 Eq, 11 mmol). In a separate vial, dibenzo[b,d]thiophene (1.0 g, 1 Eq, 5.4 mmol) was measured out and DCM (10 mL) was added. The activated solution of dibenzothienophene in DCM was then added dropwise to the solution of activated acetyl chloride. The reaction stirred at 40°C for 6 hours and yielded (a) and the diacylated byproduct (b). A column was run from 0-100% DCM in Hexane. Starting material was recovered at around 30% DCM- Hexane. The diacylated product (b) came out first at around 40% DCM-Hexane. The column was run at 40% DCM-Hexane for at least 300mL. The product also began to come out at about 40% DCM-Hexane. After just the product was leaving the column, the solvent system was gradually increased to 100% DCM to finish pushing the product through. The product was concentrated and gave about a 58% yield of (a). Yield for the diacylated product (b) was not determined as a result of the COVID-19 pandemic preventing access to the lab. ^1H NMR (400 MHz, Chloroform- d) δ 8.79 (d, J = 1.7 Hz, 1H), 8.32 – 8.25 (m,

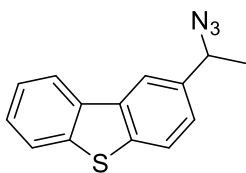
1H), 8.09 (dd, $J = 8.4, 1.8$ Hz, 1H), 7.96 (d, $J = 8.4$ Hz, 1H), 7.93 – 7.88 (m, 1H), 2.77 (s, 3H).

1-(dibenzo[b,d]thiophen-2-yl)ethan-1-ol (c)



Sodium borohydride (179 mg, 1.5 Eq, 4.74 mmol) was added to the solution of (a) in 1:1 DCM: methanol (8mL total) in a tall vial at 0°C, then stirred at RT for an hour. The crude reaction mixture was evaporated under vacuum before water and DCM were added, and the organic layer was separated, washed with H₂O, dried over anhydrous Na₂SO₄, and filtered. The organic layer was concentrated yielding the product (c) with 99% yield. ¹H NMR (400 MHz, Chloroform-*d*) δ 8.24 – 8.14 (m, 1H), 7.92 – 7.77 (m, 1H), 7.55 – 7.43 (m, 2H), 5.13 (q, $J = 6.4$ Hz, 1H), 1.63 (d, $J = 6.4$ Hz, 2H).

2-(1-azidoethyl) dibenzo[b,d]thiophene (d)



A mixture of (c) (330 mg, 1 Eq, 1.45 mmol) and diphenyl phosphorazidate (597 mg, 467 μ L, 1.5 Eq, 2.17 mmol) were suspended in dry THF in a tall vial. At 0 °C, DBU (330 mg, 327 μ L, 1.5 Eq, 2.17 mmol) was added, and the mixture was warmed to room temperature and stirred overnight (12 h). After consumption of starting material was confirmed by TLC, DCM and water were added to the crude mixture. The organic layer was separated and concentrated. A column was run from 0-100% to collect the product (d) with a 58% yield. ¹H NMR (400 MHz, Chloroform-*d*) δ 8.24 – 8.18 (m, 1H), 8.14 (d, $J = 1.8$ Hz,

1H), 7.93 – 7.83 (m, 2H), 7.54 – 7.48 (m, 2H), 7.46 (dd, $J = 8.3, 1.8$ Hz, 1H), 4.85 (q, $J = 6.8$ Hz, 1H), 1.67 (d, $J = 6.8$ Hz, 3H).